PREDICTION OF TRANSONIC BUFFET ONSET FOR FLOW OVER A SUPERCRITICAL AIRFOIL- A NUMERICAL INVESTIGATION

Arif Abdullah Rokoni and **A.B.M. Toufique Hasan***
Department of Mechanical Engineering
Bangladesh University of Engineering and Technology (BUET), Dhaka-1000, Bangladesh
*Corresponding e-mail: toufiquehasan@me.buet.ac.bd

Abstract: *Transonic flow over a supercritical airfoil leads to the appearances of unsteady shock waves in the flow field. At certain flow conditions, the interaction of unsteady shock waves with boundary layer becomes complex and generates self-excited shock oscillation, lift fluctuation and thus initiate the buffet. In the present study, Reynolds averaged Navier-Stokes equations with k-ω SST turbulence model has been applied to predict the shock induced buffet onset for the flow over a supercritical airfoil NASA SC(2) 0714. The free stream transonic Mach number is kept in the range of 0.71 to 0.75 while the angle of attack is varied in a wide range. The onset of buffet is confirmed by the fluctuating aerodynamic properties such as lift-coefficient, pressure coefficient, static pressure and so on. The self-excited shock oscillation and the corresponding buffet frequency are numerically analyzed.*

Keywords*: transonic flow, shock oscillation, buffet, numerical simulation*

INTRODUCTION

The transonic flow over an airfoil is associated with the appearance of unsteady shock waves which interact strongly with the boundary layer. At a given free-stream Mach number and for small angle of attack, the flow reattaches; while at sufficient high angles of attack, the boundary layer separates either as a bubble at the foot of the shock or at the trailing edge (Crouch et al., 2009; Lee, 2001). At particular transonic flow conditions, the self-excited shock oscillates alternatively along the airfoil surfaces. This large-scale flow-induced shock motion is known as shock buffet which is potentially detrimental for aerodynamic structure as well as the safe operation of turbomachinery .

Several computational and experimental studies showed that the buffet onset is influenced by the geometry and trailing edge viscous-inviscid interaction. Lee (1990) proposed a feedback mechanism for self-excited shock motion on a supercritical airfoil. On the other hand, prominent features of the shock buffet of the 18-percent-thick circular-arc airfoil have been computed by Gillan (1995) and Rumsey *et al.* (1995) with Navier-Stokes and thin-layer Navier-Stokes codes, repectively. These computations highlighted the sensitivity of this type of problem to the turbulence and the flow modeling and the importance of shock and trailing-edge separation. However, these studies have determined the range of Mach number for the onset of shock buffet for the circular-arc airfoil quite accurately. However, the physical mechanism for buffet onset is still not fully well established.

Mabey *et al*. (1981) investigated the physical mechanisms of buffet onset for the case of 14-percent circular-arc airfoil considering the shock strength ahead of the shock wave. Geometry and trailing-edge viscous-inviscid interaction played a role as well. In case of 18-percent circular-arc airfoil, trailing edge separation has observed prior to shock induced separation and shock buffet onset (Chen *et al*., 2010; McDevitt *et al*.,1981; Tijdeman and Seebass, 1980). Shock oscillation is antisymmetric and hysteresis occurs at the range of onset Mach number for this airfoil (Edwards,1993). However, NACA 0012 airfoil has a weaker trailing edge separation in its buffet onset region (Bartels, 1998). This airfoil shows one-sided shock buffet though the geometry is symmetric. This airfoil has no sensitivity on Reynolds number in its buffet onset regions and does not show any hysteresis effect at all unlike other circular arc airfoil. Though supercritical airfoils are introduced to increase the drag divergence Mach number and thus to extend the buffet boundary, several experiments showed that these airfoils also experience the shock buffet at flight conditions (Bartels, 1998, Deck, 2005, Xiao *et al*., 2006). Xiao *et al*. (2006) numerically investigated the transonic buffet over a Bauer–Garabedian–Korn (BGK) No. 1 supercritical airfoil. Two steady cases (M= 0.71, α = 1.396 deg and M = 0.71, α = 9.0 deg) and one unsteady case (M= 0.71, α= 6.97 deg) were analyzed in detail. Space-time correlations of the unsteady pressure field were used to calculate the time for pressure waves to travel downstream within the separated region from the shock wave to the airfoil trailing edge and then back from the trailing edge to the shock outside the separated region. The reduced frequency so calculated agreed well with the computed buffet frequency.

In the present study, the Reynolds averaged Navier-Stokes equations with k-ω SST (Shear Stress Transport) two equation turbulence model is applied to predict the shock induced buffet onset over a supercritical airfoil NASA SC(2) 0714. The fee stream transonic Mach number is kept in the range of 0.71 to 0.75. The computational data first have been validated using the experimental data from high

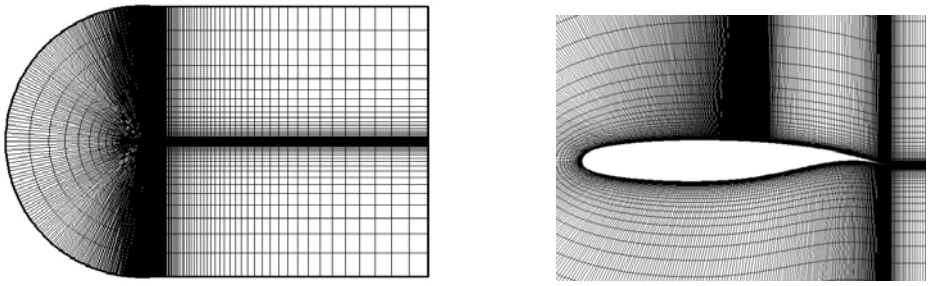

(a) (b)

Figure 1. (a) Computational domain with grids; (b) Closed-up view of grids around NASA SC(2) 0714 Airfoil

Reynolds number wind tunnel test conducted in the Langley 0.3-Meter Transonic Cryogenic Tunnel (Bartels and Edwards, 1997). The critical point at which buffet onset occurs has been predicted by increasing the angle of attack by an increment of 0.10°. Buffet onset is determined by the appearance of fluctuating aerodynamic properties such as lift coefficient, pressure coefficient and static pressure at particular combination of flow conditions. A detailed analysis on the buffet flow together with the large scale self-excited shock oscillation are investigated for the range of transonic Mach numbers. The dominant frequency of shock oscillation is also determined in this study.

NUMERICAL MODELLING

The flow in this study is considered to be viscous, compressible, turbulent, and unsteady. Governing equations for the present RANS computations are the conservation of mass, conservation of momentum and the energy equations written in 2-D coordinate system. Two additional transport equations of k-ω SST (Shear Stress Transport) turbulence model are included to model the turbulence in the flow field. The governing equation can be written in the following vector form:

$$\frac{\partial \boldsymbol{U}}{\partial t}+\frac{\partial \boldsymbol{E}}{\partial x}+\frac{\partial \boldsymbol{F}}{\partial y}=\frac{\partial \boldsymbol{R}}{\partial x}+\frac{\partial \boldsymbol{S}}{\partial y}+\boldsymbol{H} \qquad (1)$$

Here $\boldsymbol{U}$ is the conservative flux vector. $\boldsymbol{E}$ and $\boldsymbol{F}$ are the inviscid flux vectors and $\boldsymbol{R}$ and $\boldsymbol{S}$ are the viscous flux vectors in the x and y directions, respectively. $\boldsymbol{H}$ is the source terms corresponding to turbulence.

The governing equations are discretized spatially using a Finite volume method of second order scheme. For the time derivatives, an implicit multistage time stepping scheme, which is advanced from time t to time $t+\Delta t$ with a second order Euler backward scheme for physical time and implicit pseudo-time marching scheme for inner iteration, is used. A time step size of 10^{-5} was sufficient for this type of unsteady computation..

The computational domain together with the grids are shown in Fig. 1(a). The chord length c of NASA SC(2) 0714 supercritical airfoil is considered to be 152.4 mm. The upstream and downstream boundaries are located at 11.5c and 21c, from the leading edge of the airfoil. On the other hand, the top and bottom boundaries are 12.5c apart from the airfoil surfaces. This spacing was considered to be sufficient to apply free-stream conditions on the outer boundaries. The adiabatic no-slip conditions are applied to airfoil surfaces. The Reynolds number based on the airfoil chord length, Re = 2.50×10^6, 2.54×10^6, 2.57×10^6, 2.61×10^6, 2.64×10^6 for M_∞ = 0.71, 0.72, 0.73, 0.74 and 0.75, respectively.

A structured clustered grid system using quadrilateral cells was employed in the computations. The total number of grids is 51,000 which gives a grid independent solution. For viscous flow calculation, extra fine spaced grids was constructed over the airfoil surfaces as shown in Fig. 1(b). The first point above the airfoil surface is located at 0.0000169c from the airfoil surface which corresponds to $y^+ < 1$. A solution convergence was obtained when the residuals for each of the conserved variables were reduced below the order of magnitude 5.

COMPUTATIONAL VALIDATION

Before going to the detail discussion of the present problem, the computational results have been validated with the available experimental data. Computational validation has been performed by comparing pressure coefficients over the supercritical airfoil for three different conditions. Experimental results are obtained from Ref. (Bartels and Edwards, 1997).

Figure 2 shows the distribution of pressure coefficient, c_p along the airfoil surfaces obtained both from the experiments and the computations for different buffet conditions. The open square symbols are the experimental data and the closed circles are the computational results. In general the trend of c_p are same along the airfoil surfaces both from experiment and the computations. The positions of the shock wave are also at the identical positions for both experimental and computational cases. However, for M_∞ = 0.72, $\alpha = 2.5^{\circ}$, computational results are showing larger pressure drop than the

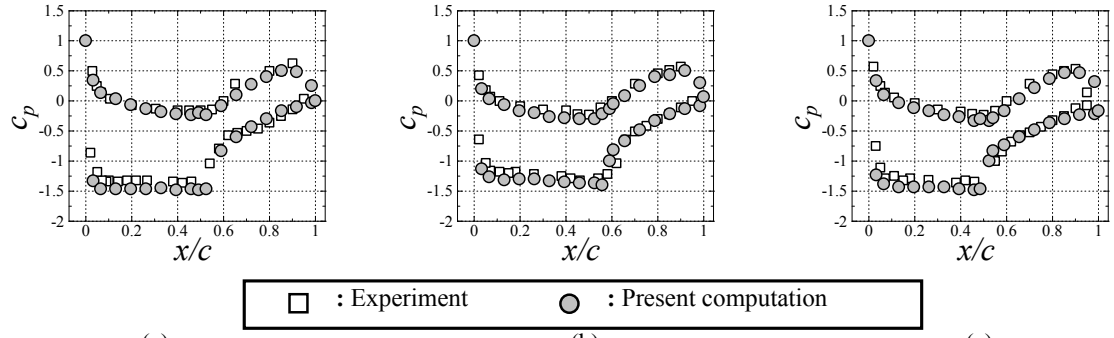

(a) (b) (c)

Figure 2. Distribution of pressure coefficient along the airfoil surfaces; (a) $M_\infty = 0.72$, $\alpha = 2.5^o$; (b) $M_\infty = 0.74$, $\alpha = 2.0^o$ and (c) $M_\infty = 0.74$, $\alpha = 3.0^o$.

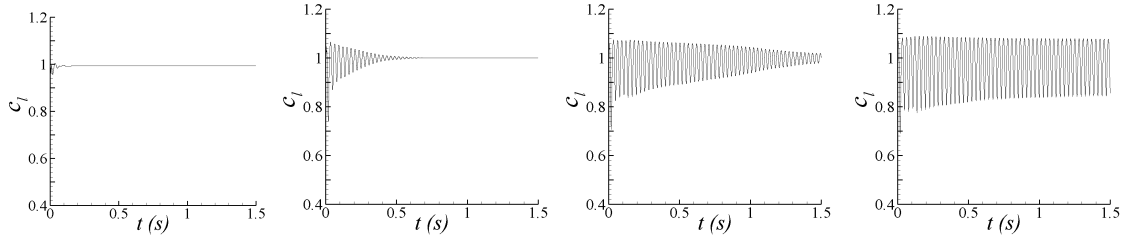

(a) (b) (c) (d)

Figure 3. Evolution of lift coefficient at $M_\infty = 0.71$; (a) $\alpha = 3.0^o$, (b) $\alpha = 3.5^o$, (c) $\alpha = 3.6^o$, and (d) $\alpha = 3.7^o$.

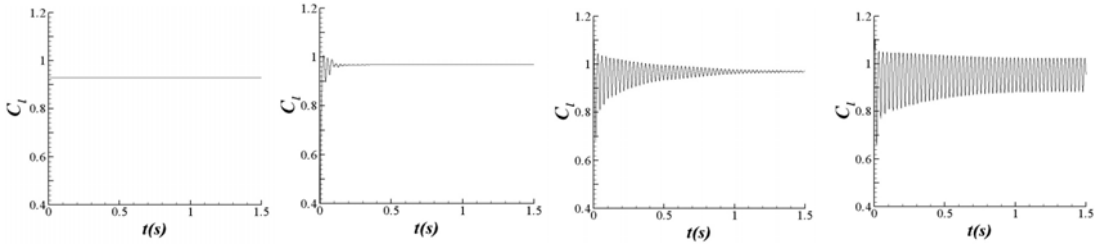

(a) (b) (c) (d)

Figure 4. Evolution of lift coefficient at $M_\infty = 0.72$; (a) $\alpha = 2.0^o$, (b) $\alpha = 3.0^o$, (c) $\alpha = 3.2^o$, and (d) $\alpha = 3.3^o$.

experimental values on the upper surface of the airfoil as shown in the Fig 3 (a). However, a good relation exists between the experiment and present computational results for other conditions as shown in Figs. 3(b) and 3(c).

RESULTS AND DISCUSSION

Present computation starts with a known steady state combination of Mach number, M_∞ and angle of attack, α far below the buffet onset. Then the unsteady calculation proceeds by increasing the angle of attack in small step like 0.1°. To identify the shock induced oscillations the lift coefficient convergence history and static pressure-time history at various points near the airfoil upper surface have been examined.

Figure 3 shows the evolution of lift coefficient at $M_\infty = 0.71$ for different angles of attack, α. Results are shown up to time of 1.5s. At this free stream condition, the lift coefficients are initially oscillates and subsequently damped out for $\alpha = 3.0^o$, 3.5^o, 3.6^o as shown in Figs. 3(a), 3(b) and 3(c), respectively. The flows computed at these angles of attack are came to a stabilized condition with the advancement of time. There are no oscillations associated with numerical instability. Moreover, the flows are not totally separated in a manner to shed the trailing edge vortices. However, with an increase of angle of attack of 0.1^o from 3.6^o to 3.7^o, a stable oscillation of lift coefficient without damping is observed as shown in Fig. 3(d). This angle of attack can primarily be considered as the buffet onset for $M_\infty = 0.71$. At this condition, the amplitude of undamped lift coefficient oscillation is about 15% of the magnitude of average lift coefficient. This consideration is kept the same for all the cases discussed below.

Figure 4 shows lift coefficient evolution at $M_\infty = 0.72$ for different angles of attack. Beyond $\alpha = 3.3^o$, lift coefficients are initially oscillating followed by damping and became steady with the advancement of time. At $\alpha = 3.3^o$, a stable oscillating lift distribution with time is observed. Thus $\alpha = 3.3^o$ is the onset of buffeting flow for $M_\infty = 0.72$.

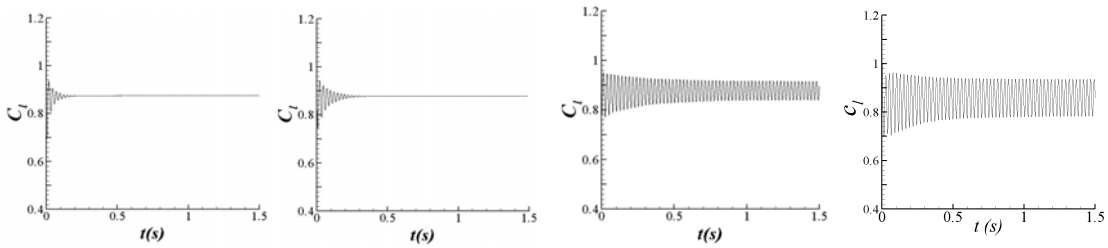

(a) (b) (c) (d)

Figure 5. Evolution of lift coefficient at $M_\infty = 0.74$; (a) $\alpha = 2.5^o$, (b) $\alpha = 2.6^o$, (c) $\alpha = 2.8^o$, and (d) $\alpha = 2.9^o$

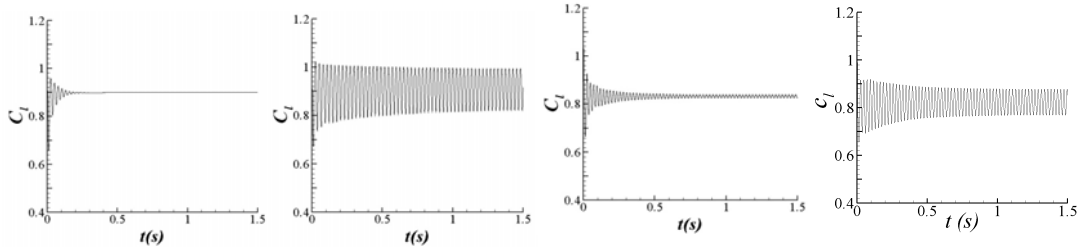

(a) (b) (c) (d)

Figure 6. Evolution of lift coefficient at (a) M_∞=0.73 , $\alpha = 3.0^o$, (b) $M_\infty = 0.73$, $\alpha = 3.1^o$, (c) $M_\infty = 0.75$, $\alpha = 2.7^o$, (d) M_∞=0.75 , $\alpha = 2.8^o$.

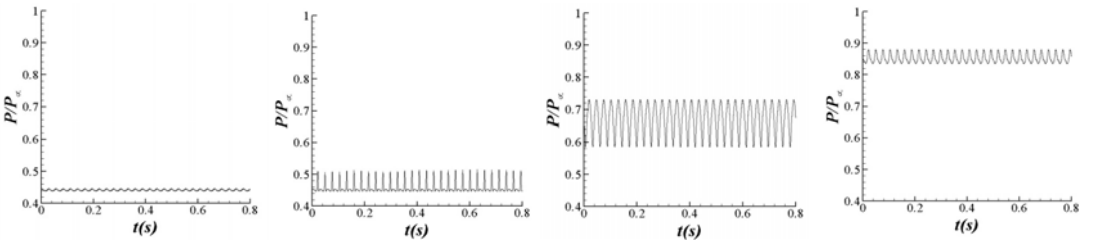

(a) (b) (c) (d)

Figure 7. Static pressure time histories at the upper surface of the airfoil for $M_\infty = 0.73$, $\alpha = 3.1^o$; (a) x/c=0.1, (b) x/c=0.3, (c) x/c=0.5, and (d) x/c=0.7.

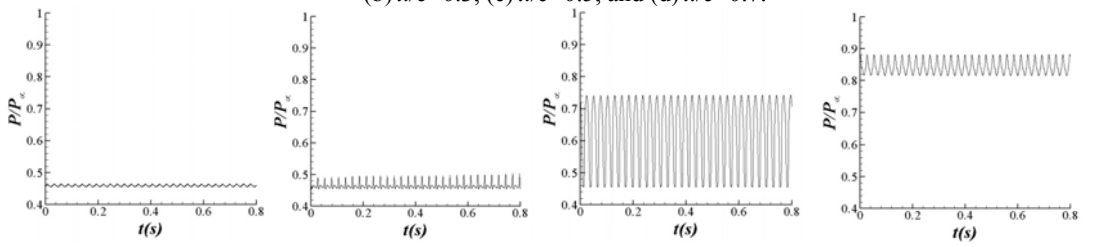

(a) (b) (c) (d)

Figure 8. Static pressure time histories at the upper surface of the airfoil for $M_\infty = 0.74$, $\alpha = 2.9^o$; (a) x/c=0.1, (b) x/c=0.3, (c) x/c=0.5, and (d) x/c=0.7.

For $M_\infty = 0.74$, buffet onset is at $\alpha = 2.9^o$ which is confirmed with the above consideration as shown in Fig. 5. Lift coefficients for other flow conditions of $M_\infty = 0.73$ and $M_\infty = 0.75$ are shown in Fig. 6. Results are presented for angles of attack just before the buffet onset and at the start of buffet. It is found that the buffet onset is observed at $\alpha = 3.1^o$ and $\alpha = 2.8^o$ for $M_\infty = 0.73$ and 0.75, respectively.

To further confirm the onset of buffeting flow, time histories of local static pressure are considered. The time histories of static pressures have been shown for buffet onset angle for Mach numbers of 0.73 and 0.74 as shown in Figs. 7 and 8, respectively for brevity. The location of maximum shock induced unsteadiness is observed at $x/c = 0.5$. However, at this location ($x/c = 0.5$), a rise in amplitude of pressure oscillation is observed for $M_\infty = 0.73$ and $M_\infty = 0.74$ compared to $M_\infty = 0.72$.

From the above aerodynamic behavior, the buffet onset boundary is clearly identified for NASA SC(2) 0714 airfoil in the transonic Mach number ranges of 0.71 to 0.75 as shown in Fig. 9. This figure

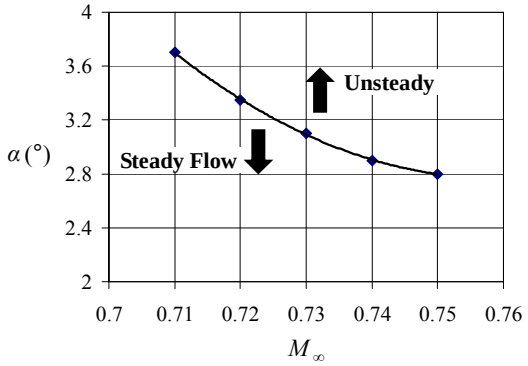

Figure 9. The Buffet onset boundary for NASA SC(2) 0714

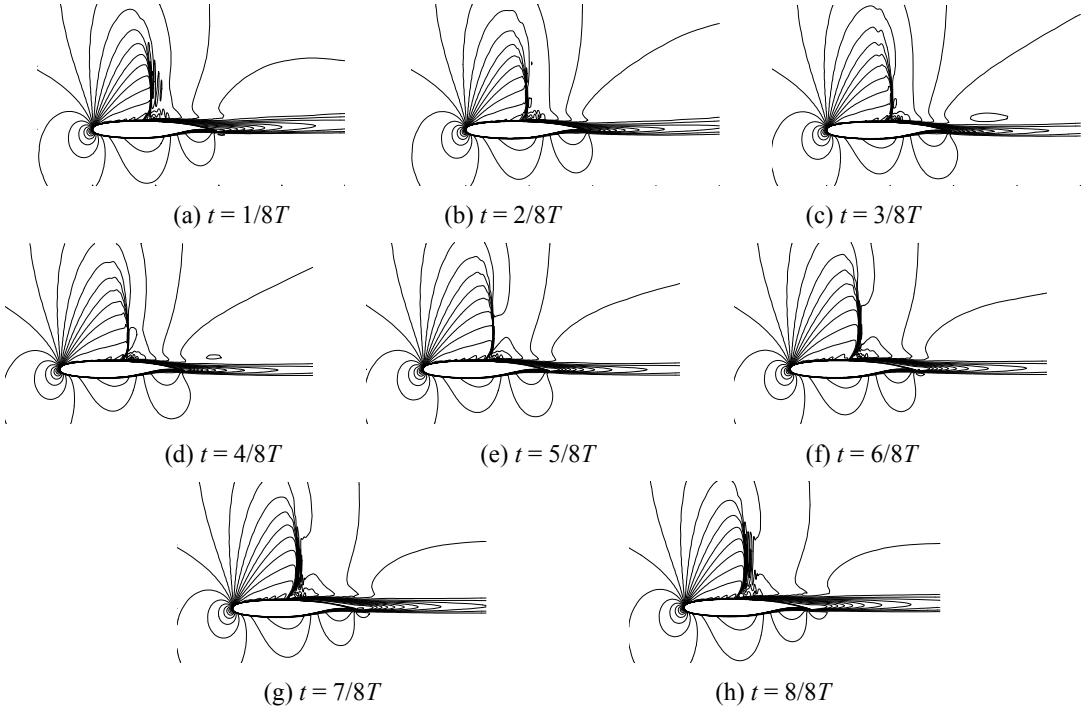

Figure 10. Sequential contour maps of Mach number around NASA SC(2) 0714 supercritical airfoil at $M_\infty = 0.72$, $\alpha = 3.3^o$

clearly distinguish the regime of steady flow and unsteady buffet. Moreover, buffet onset boundary decreases with an increase of free stream Mach number, M_∞. This is due to the increase of shock Mach number and subsequent intensification of shock induced boundary layer separation at higher Mach numbers, M_∞.

The flow field characteristics at the buffet onset angle for Mach number of 0.72 is shown in Fig. 10. The frequency of shock oscillation is around 36.6 Hz corresponding to the time period, T of 0.027s. Eight snapshots have been shown during one period of shock oscillation in Fig. 10. It is found that the shock oscillates around the airfoil upper surface only. In this case, shock wave starts to oscillate from x/c = 0.4 at $t = 1/8T$ (Fig. 10(a)) and reaches the maximum rearward position at $x/c = 0.5$ at $t = 4/8T$ (Fig. 10(d)). During this rearward movement, shock strength is slightly reduced and thus the intensity of shock induced boundary layer separation. After that, shock starts to move forward from $x/c = 0.5$ at $t = 4/8T$ (Fig. 10(d)) and reaches the maximum forward position at $x/c = 0.4$ at $t = 8/8T$ (Fig. 10(h)) and thus completes the cycle. During the forward motion, the shock strength successively increased and showed higher shock induced boundary layer separation compared to rearward motion. At this flow conditions, the shock excursion length is about 10% of the chord length. This shock motion involves alternating separation and reattachment of the boundary layer. This is a viscous phenomenon and occurs solely due to unsteady interaction of shock wave with boundary layer.

Table 1: Buffet frequency, f_{buffet} at different flow condition

M_∞ (-)	0.71	0.72	0.73	0.74	0.75
f_{buffet} (Hz)	36.6	36.1	35.9	35.5	35.2

The computed frequencies of shock oscillation at buffet boundary for transonic flow around the supercritical airfoil NASA SC(2) 0714 are shown in Table 1.

CONCLUSIONS

Reynolds averaged Navier-Stokes equations together with k-ω Shear Stress Transport turbulence model has been employed to predict the shock induced buffet boundary for transonic flow over a NASA SC(2) 0714 supercritical airfoil. Prediction of such boundary for supercritical airfoil is numerically very challenging as this type of airfoil has a much strong viscous-inviscid interaction behind the shock than the conventional airfoil. However, the computational results of pressure coefficients on both upper and lower surfaces of the airfoil have been compared with the experimental data for the integrity of the present numerical technique. The results obtained from the present numerical computations can be summarized as follows:

- Shock induced buffet boundary is determined based on the angle of attack for the free stream transonic Mach number range of 0.71 to 0.75.
- At buffet onset, a low frequency and large scale shock oscillation has been observed on the upper surface of the supercritical airfoil.
- The shock oscillation is self excited at and beyond the buffet onset.
- At these conditions, unsteady shock interaction with the boundary layer has been captured and confirmed by the fluctuating static pressure time histories at successive streamwise locations along the airfoil upper surface.

REFERENCES

[1] Crouch, J. D., Garbaruk, A., Magidov, D., Travin, A., 2009, Origin of transonic buffet on aerofoils, *Journal of Fluid Mechanics*, 628, pp. 357-369.

[2] Lee, B. H. K., 2001, Self-sustained shock oscillations on airfoils at transonic speeds, *Progress in Aerospace Sciences*, 37(2), pp.147-196.

[3] Lee, B. H. K., 1990, Oscillatory shock motion caused by transonic shock-boundary interaction, *AIAA Journal*, 28, pp. 942-944.

[4] Gillan, M. A., 1995, Navier-Stokes simulation of self-excited shock induced oscillations", *AIAA- 95-1809.*

[5] Rumsey, Christopher L., Sanetrick, Mark D., Biedron, Robert T., Melson, N. Duane, Parlette, Edward B. , 1995, Efficiency and accuracy of time-accurate turbulent Navier-Stokes computations, *Proc. of the 13th AIAA Applied Aerodynamics Conference*, AIAA-95-1835.

[6] Mabey, D. G., Welsh, B. L. and Cripps, B. E. , 1981, Periodic flows on a rigid 14% thick biconvex wing at transonic speeds, *RAE-TR-81059*.

[7] Chen, L.W., Xu, C.Y., Lu, X.Y., 2010, Numerical investigation of compressible flow past an aerofoil, *Journal of Fluid Mechanics*, 643, pp. 97-126.

[8] McDevitt, J. B.; Levy, L. L., Jr.; and Deiwert, G. S., 1976, Transonic flow about a thick circular-arc airfoil, *AIAA Journal*, 14, pp. 606-613.

[9] Tijdeman, H., Seebass, R., 1980, Transonic flow past oscillating airfoils, *Annual Review of Fluid Mechanics*, 12, pp. 181-222.

[10]Edwards, J. W., 1993, Transonic shock oscillations calculated with a new interactive boundary layer coupling method, *AIAA-93-0777*.

[11]Bartels, R. E., 1998, Flow and turbulence modeling and computation of shock buffet onset for conventional and supercritical airfoils. *NASA TP-1998-206908*.

[12]Deck, S., 2005, Numerical simulation of transonic buffet over a supercritical airfoil, *AIAA Journal*, 43, pp. 1556-1566.

[13]Xiao, Q., Tsai, H., Liu, F., 2006, Numerical study of transonic buffet on a supercritical airfoil, *AIAA Journal*, 44, pp. 620-628.

[14]Bartels, R., E, and Edwards, J. W., 1997, Cryogenic tunnel pressure measurements on a supercritical airfoil for several shock buffet conditions, *NASA TM-110272.*